Combined synchrotron X-ray diffraction, dilatometry and electrical resistivity in situ study of phase transformations in a Ti2AlNb alloy

V.A. Esin, R. Mallick, M. Dadé, B. Denand, J. Delfosse, P. Sallot

Version of Record: https://www.sciencedirect.com/science/article/pii/S1044580320321252
Manuscript_fbabe35d0c9abcf9729ea4857849aa85

Combined synchrotron X-ray diffraction, dilatometry and electrical resistivity in situ study of phase transformations in a Ti2AlNb alloy

V.A. Esin*[1], R. Mallick[1,2], M. Dadé†[1], B. Denand[3], J. Delfosse[2], and P. Sallot[2]

[1]MINES ParisTech, PSL University, Centre des Matériaux (UMR CNRS 7633), Évry, France
[2]Safran Tech, Magny-les-Hameaux, France
[3]Institut Jean Lamour, Unversité de Lorraine, Nancy, France

September 9, 2020

Abstract

Phase transformations in near Ti2AlNb alloy occurring on cooling of 10 °C min^{-1} from 1020 °C were studied in situ using high energy X-ray diffraction and electrical resistivity measurements coupled with simultaneous dilatometric analysis. From Rietveld refinement of X-ray data, it was established that high temperature range from about 870 to 1020 °C contained partially ordered β phase. The degree of long-range order was of 0.6 at 1020 °C and decreased slowly with temperature decrease and fast when O-phase was formed. The formation of O-Ti_2AlNb phase started from about 870 °C and consisted of two stages: (i) fast transformation of partially ordered β into O phase at higher temperatures followed by (ii) slow transformation of fully disordered β into O-phase at lower temperatures. The appearance of O-phase was accompanied by important volume decrease of the alloy as recorded using dilatometry as well as by a decrease of electrical resistivity. The transformations temperatures revealed by high energy X-ray diffraction, dilatometry and electrical resistivity were in good agreement. The obtained results were discussed using thermodynamic simulations carried out with Thermo-Calc software and TCTI2 database.

Keywords: Ti_2AlNb alloy; phase transformation; ordering; synchrotron; electrical resistivity; dilatometry

*Corresponding author: V.A. Esin (vladimir.esin@mines-paristech.fr)
†Presently at Eramet Ideas, Trappes, France

1 Introduction

In modern aeroengines parts made of Ti-based alloys can represent up to 30% of their weight, which makes these alloys the second most used material behind Ni-based superalloys [1]. For instance, high-pressure compressors contain near-α Ti alloys on their first stages and Ni-base superalloys for the stages where the service temperatures exceed 500 °C.

One effective way to improve the overall efficiency of aeroengines is to decrease their weight. Therefore, the substitution of parts currently made of Ni-base superalloys (density 8-9 g cm^{-3}) by lightweight materials in areas where the service temperature is below 650 °C would be a possible issue. For the moment, conventional Ti-based alloys suffer from a dramatic degradation of their mechanical properties and their oxidation resistance at temperatures higher than 500 °C, making Ni-base superalloys the only reliable solution.

In this scope γ-TiAl alloys having good oxidation resistance together with good mechanical properties at high temperature were developed and introduced on last generations of aeroengines on low pressure turbine blades [1]. They possess lower density, better creep properties, increased Young's modulus and corrosion resistance as compared to conventional near-α Ti-base alloys. However, their low ductility at room temperature, low toughness and low crack propagation resistance limit their applications.

In 1960s McAndrew reported a beneficial effect of Nb addition on ductility of α_2-Ti_3Al alloys [2]. Such a result led to appearance of new class of Ti-based alloys intended to overcome the drawbacks of γ-TiAl alloys keeping good oxidation resistance. It is based on generic composition of Ti2AlNb resulting in the formation of the orthorhombic phase O-Ti_2AlNb discovered by Banerjee et al. [3]. This phase is usually formed below 950 °C from high temperature cubic β and/or α_2 phases well known in conventional Ti-based alloys. The O-Ti_2AlNb phase has a good creep resistance and better ductility than α_2 phase. Two-phase β+O and three-phase β+α_2+O alloys have good mechanical properties at high temperature and low density as compared to current Ni-base superalloys actually used [1, 4]. Moreover, they possess better oxidation and fire resistance than conventional Ti-based alloys.

Since their discovery, the phase stability in Ti2AlNb alloys have been studied with a particular attention to the effect of chemical composition [5, 6] or/and heat treatment [7–10]. It is now well established that cubic β phase alone is stable at high temperatures and α_2 appears in the intermediate temperature range (from 1050 to 800 °C depending on the alloy composition). Both β and α_2 transform into O phase when the temperature decreases and the transformation can be diffusion controlled [6, 11], massive [3, 6, 12] or even martensitic [5–7]. Two types of O phase, O1 and O2, were suggested depending on the temperature [12].

The majority of studies carried out to date on phase transformations in Ti2AlNb alloys were performed using conventional characterization methods (heat treatment followed by quenching and observations/characterizations at room temperature) which required a hypothesis that no transformation occurred on quenching and observed microstructure corresponded thus to high temperature domain. An in situ characterization was attempted by Sadi et al. [13] who used dilatometry, calorimetry and electrical resistivity measurements to follow the phase transitions occurring on heating and on cooling in a near Ti2AlNb alloy. Even though these techniques allowed to study the phase transformations in real time, complementary *post mortem* analyses were required to interpret the data and, namely, to identify the nature of different phases involved in the phase transformations. Due to these experimental uncertainties, there still exists a confusion on ordering of high temperature β phase which was reported to be completely ordered [3, 5, 8, 12–15] or partially ordered [7, 16, 17]. The use of in situ characterization at high temperature could help to clarify this point. Therefore, detailed understanding of phase transformation mechanisms is quite limited for Ti2AlNb alloys and mostly restricted to ternary or quaternary compositions. The strong dependency of mechanical properties as well as oxidation resistance on the microstructure underlines the importance of detailed understanding of mechanisms operating during different steps of production route [9, 10, 18, 19]. Therefore, the present study reports the results obtained using in situ high-energy X-ray diffraction (HE-XRD) experiments to follow the phase transitions on cooling in a Ti2AlNb alloy with Zr, Mo and Si additions to increase mechanical prop-

erties [20, 21]. Recently, high-energy X-ray diffraction was successfully applied to study complex phase transformations in γ-TiAl alloys enriched in Nb [22–24]. However, to the best of our knowledge, such a technique remains rarely used for Ti2AlNb alloys.

2 Material and methods

2.1 Studied Ti2AlNb alloy

The chemical composition of used Ti2AlNb alloy is given in Table 1. For the present study, the alloy was produced by vacuum induction melting (VIM) followed by vacuum arc remelting (VAR) by GfE (Germany). Hot extrusion was carried out by Cefival (France) in the temperature range corresponding to β phase domain using an as-cast ingot. It was followed by a two-step forging and a sequence of isothermal heat treatments to produce a typical microstructure consisting of O, β and α_2 phases [12, 25]. The objective of the present work was to follow the phase transitions on cooling from the high temperature domain. Therefore, before the experiments, the alloy was rehomogenized at 1020 °C during 1 hour and water quenched and a single-phase microstructure consisting of β grains was observed using scanning electron microscope (SEM) (Figure 1).

Table 1: Chemical composition (at. %) of studied Ti2AlNb alloy

Ti	Al	Nb	Mo	Zr	Si	O*	N*	H*
bal.	23-24	21-22	1.5-2	1-1.5	0.2-0.3	660	40	20

*en wt. ppm.

2.2 Heat cycle

The sequence of phase transformations on cooling was followed in situ using high-energy X-ray diffraction, electrical resistivity measurements as well as dilatometric analysis. It is worth noting that for in situ X-ray diffraction and electrical resistivity experiments different furnaces were used for the heat cycle. Nevertheless, since the dilatometric curves were recorded for both X-ray diffraction and electrical resistivity measurements, it allowed

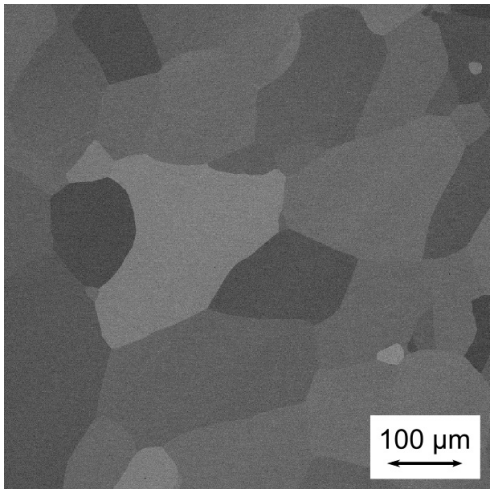

Figure 1: Initial microstructure of studied Ti2AlNb alloy consisting of β grains observed using scanning electron microscope (backstcattered electrons).

to conclude on the reliability of results obtained by the different techniques.

The heat cycle consisted of fast heating of 60 °C s^{-1} from room temperature to 1020 °C to avoid any phase transformation on heating, holding at 1020 °C for 5 minutes for temperature homogenisation and cooling to 550 °C with a rate of 10 °C min^{-1} to study the sequence of phase transformations followed by Ar quenching.

2.3 X-ray diffraction analysis

X-ray diffraction experiments were carried out at P07 beamline of PETRA III at DESY (Deutsches Elektronen Synchrotron, Hamburg, Germany). Induction heating using Bähr DIL805 A/D dilatometer was used to perform the heat treatment described above. The temperature was controlled by Pt/Pt-Rh thermocouple spot-welded on the surface at the center of the sample in the zone of X-ray analysis to get precise temperature values during in situ heating [26]. The experiments were carried out under vacuum of 10^{-4} mbar.

A monochromatic beam of 100 keV was used to perform X-ray diffraction analysis in a transmission mode. 2D X-ray detector was placed ≈1.5 m away from the sample; the exact distance from the sample to the detector was determined using LaB_6 powder standard. Since X-ray wavelength was of 0.123984 Å, the diffraction angles were smaller than 10°. The acquisition time of each diffractogram was of 3.5 s and included the shutter opening, acquisition of external parameters (temperature, beam characteristics), shutter

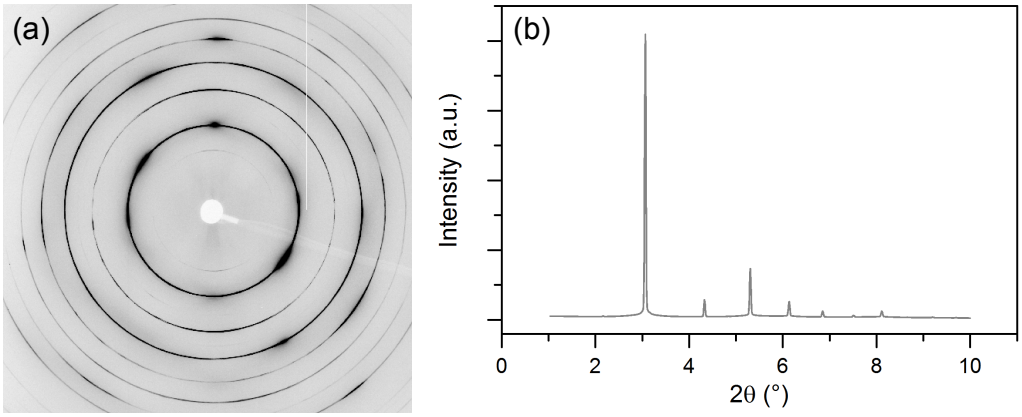

Figure 2: Diffractograms obtained during in situ heat treatment at the end of holding at 1020 °C: (a) as acquired 2D diffractogram and (b) 1D diffractogram after circular integration using FIT2D software.

closure and data erasing from 2D detector for the next acquisition.

An example of as acquired 2D diffractogram showing obtained Debye-Scherrer rings at the end of isothermal holding at 1020 °C is given in Figure 2a. One can observe several intense spots indicating a slight texture or/and large grains in the studied sample. To perform Rietveld refinement [27], 2D diffractograms were integrated using FIT2D software [28] to obtain standard 1D diffractograms (Intensity *vs.* diffraction angle 2θ) (Figure 2b).

In a typical Ti2AlNb alloy, phases such as β, α_2 and O-Ti_2AlNb are expected to form. Moreover, two distinct ordered O phases, O1 and O2, can exist [12]. Therefore, possible formation of all these phases on cooling should be taken into account during Rietveld refinement of obtained X-ray data. It is worth noting, that the analysis carried out in the present work did not reveal the appearance of diffraction peaks corresponding to α_2 phase. The reasons for such an unexpected result will be discussed further. Moreover, no indication of coexistence of two different types of O phase was observed neither. Therefore, Rietveld refinement of diffractograms was carried out taking into consideration β and O phases only.

β phase is the high temperature bulk centered cubic structure of Ti [29] which can be partially ordered, according to B2 structure, where Ti and Al/Nb occupy different crystalline sites [30]. The O-Ti_2AlNb is orthorhombic phase [31]. The space groups and

Table 2: Crystalline data for β and O-Ti_2AlNb phases considered in the present study as well as occupation factors and ATZ parameter taken for Rietveld refinement using FullProf software.

Phase	Space group	Atom	Wyckoff notation	Site coordinates			Reference	Parameters for Rietveld refinement using FullProf	
				x	y	z		Occupation factor[2]	ATZ[3]
β[1]	$Pm\bar{3}m$	Ti	1(a)	0	0	0	[30]	0.02083	107.761
		Al	1(b)	0.5	0.5	0.5		0.01042	
		Nb	1(b)	0.5	0.5	0.5		0.01041	
O	Cmcm	Al	4(c_1)	0	0.163	0.25	[31]	0.25	862.49
		Ti	8(g)	0.231	0.904	0.25		0.41150	
		Ti	4(c_2)	0	0.636	0.25		0.08850	
		Nb	8(g)	0.231	0.904	0.25		0.08850	
		Nb	4(c_2)	0	0.636	0.25		0.16150	

[1]Fully ordered β phase (B2 structure) is used for Rietveld refinement to obtain the degree of long-range order, according to the procedure described in the Results section;
[2]Occupation factor in FullProf software is a product of ratio site multiplicity/general multiplicity and site occupation [32];
[3]ATZ is a parameter required for quantitative phase analysis, ATZ=ZM, where Z is number of formula units per cell and M is a molecular weight [32].

atomic positions for β and O phases considered in the present study are given in Table 2. For the β phase, fully ordered B2 structure was taken for Rietveld refinement to be able to obtain the degree of long-range order, according to the procedure described in the Results section.

Rietveld refinement was carried out using FullProf software (version July 2017) [33]. A pseudo-Voigt function was found to give the best fit between experimental and refined diffractograms. First, the baseline (background) was adjusted manually using between 80 and 120 Intensity/2θ couples per diffractogram. Then, a number of different parameters was refined for each phase, namely, scale and shape factors, lattice parameters, full width at half maximum (FWHM) and temperature Bov factor (according to notations used in FullProf software).

2.4 Electrical resistivity measurements

Electrical resistivity during the heat cycle was measured independently of X-ray diffraction analysis. The intended heat treatment was done using a lamp furnace of a dilatometer. The electrical resistivity was followed using the four-points method [34]. The temperature was controlled by a Pt/Pt-Rh thermocouple spot-welded on the surface at the

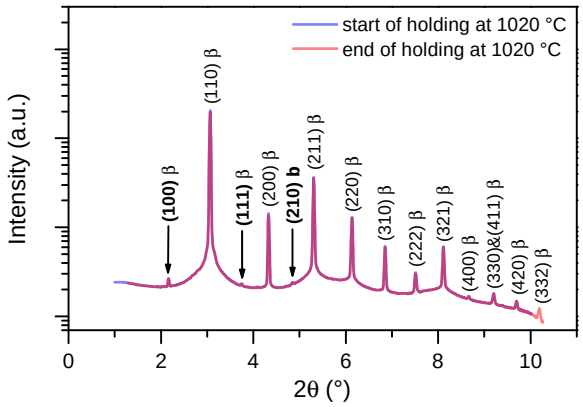

Figure 3: Diffractograms obtained at the beginning and at the end of isothermal holding at 1020 °C showing the partial ordering of β phase (the superlattice peaks are indicated in bold) (for ease of reading, logarithmic scale is used for Intensity axis).

centre of the sample. A cylindrical sample of 4 mm in diameter and 15 mm in length was used.

3 Results

3.1 Degree of long-range order of β phase

First, the sample was heated with a rate of 60 °C s^{-1} from room temperature to 1020 °C to avoid any phase transformation on heating. Remind that prior to in situ experiments using synchrotron X-ray diffraction the studied Ti2AlNb alloy had been homogenised at 1020 °C for 1 hour. The acquisition time of 3.5 s does not allow a reliable analysis of X-ray data on heating due to a significant temperature variation of 200 °C between the start and the end of each acquisition. It is worth noting however that no new diffraction ring was observed on heating.

The diffractograms obtained at the beginning and at the end of isothermal holding at 1020 °C are given in Figure 3. One can see peaks of high as well as of low intensity. Their positions and absolute intensities were not evolving during the holding revealing that phase transformations did not occur. The diffraction peaks of low intensity were found to correspond to superlattice reflections due to β phase ordering, according to B2 structure. The diffraction lines of high intensity were fundamental lines of β phase.

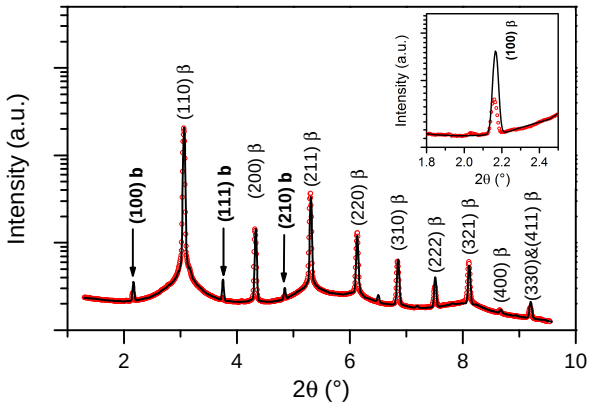

Figure 4: Rietveld refinement (black solid) of experimental diffractogram (red, open circles) obtained at the end of isothermal holding at 1020 °C using fully ordered β phase (B2 structure). The inset highlights the difference between calculated and measured intensity of (100) diffraction peak indicating partial ordering of β phase (for ease of reading, logarithmic scale is used for Intensity axis).

To determine the degree of long-range order of β phase, each diffractogram was refined applying Rietveld method using FullProf software (Figure 4). At the end of isothermal holding at 1020 °C, and before the cooling, the studied alloy only contained partially ordered β phase; the ordering is revealed by the presence of so-called superlattice diffraction peaks (100), (111) and (210). Rietveld refinement of diffraction peaks of β phase was carried out using completely ordered B2 structure consisting of 50, 25 and 25 at.% of Ti, Al and Nb, respectively (Table 2). Therefore, the minor alloying elements such as Mo, Zr and Si were neglected for simplicity.

Since the intensity of fundamental diffraction peaks is not influenced by ordering [35], a particular attention was paid to their refinement. Once the intensity of refined and experimental fundamental peaks was excellent (Figure 4), the intensity of superlattice peaks of fully ordered β phase was obtained from the calculated (refined) diffractogram. The inset in Figure 4 clearly indicates that the intensity of (100) diffraction peak of fully ordered β phase is higher than that observed experimentally suggesting thus partial ordering of β phase. Therefore, the degree of long-range order of β phase, S, can be determined by comparing the calculated intensity of (100) diffraction peak of β phase in fully ordered state, $I_{(100)}^{ordered}$, and that experimentally observed, $I_{(100)}^{exp}$, using Eq. (1) [35]:

$$S^2 = \frac{I^{exp}_{(100)}}{I^{ordered}_{(100)}} \quad (1)$$

The results show that the β phase possesses the degree of long-range ordering about 0.6 above 1000 °C and it disorders progressively when the temperature decreases and, especially, when the O-phase formation occurs, as revealed by X-ray diffraction (see the next section).

3.2 X-ray diffraction and dilatometry

The phase transformations in studied Ti2AlNb alloy were followed on cooling with a rate of 10 °C min^{-1} from 1020 to 550 °C. As detailed in the previous section, the starting phase for such a heat treatment was partially ordered β. During the cooling from 1020 to 850 °C no new diffraction peak was observed (Figure 5). However, a number of new diffraction peaks was clearly seen at 850 °C whose intensities were increasing with the decrease of temperature. At the same time, the intensity of superlattice peaks of β phase decreased and they were not detected anymore from around 800 °C (inset Figure 5).

The new peaks observed on cooling corresponded to O phase (Figure 6). It is worth noting that no diffraction peak of α_2 ($D0_{19}$) phase was detected on cooling. To obtain the evolution of the amounts of phases, Rietveld refinement of diffractograms was carried out using the crystalline properties and parameters for β and O phases given in Table 2. Therefore, the temperature dependence of phase compositions was not taken into account. An example of the refinement for diffractogram obtained at 790 °C, where β and O phases were identified, is given in Figure 6. The agreement between calculated and experimental diffractograms is good and slight differences should be associated to crystalline texture due to large initial β grains or/and to increased background stated for X-ray data.

O-phase fraction as well as the degree of long-range order of β phase for different temperatures obtained on cooling from 1020 °C with a rate of 10 °C min^{-1} are shown in Figure 7. First, the degree of ordering of β phase seemed to decrease slowly in the temperature range from 1020 to 870 °C in agreement with the decrease of intensity of superlattice diffraction peaks of β (inset in Figure 5). Then, the disordering of β phase

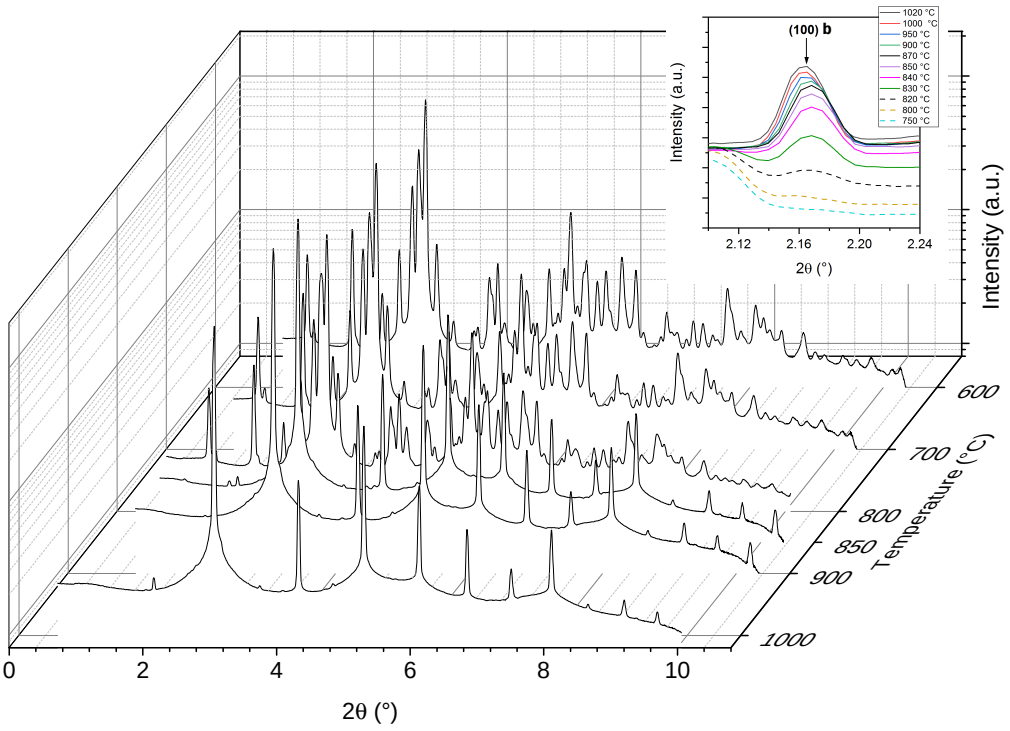

Figure 5: Diffractograms obtained during in situ cooling of 10 °C min^{-1} from 1020 to 550 °C. The inset gives the evolution of (100) superlattice diffraction peak of β phase for different temperatures (for ease of reading, logarithmic scale is used for Intensity axis).

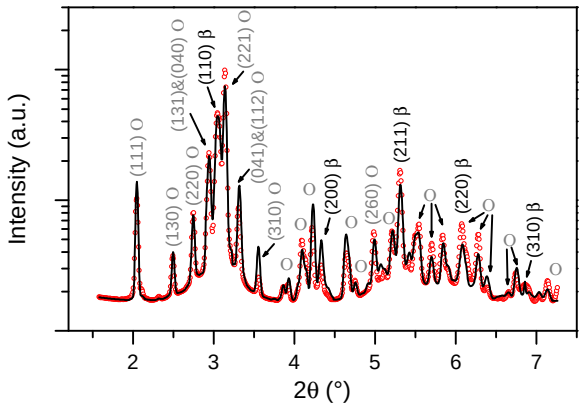

Figure 6: Example of Rietveld refinement (black solid) of diffractogram obtained at 790 °C during in situ cooling of 10 °C min^{-1} (red, open circles): peaks of β and O phases are observed.

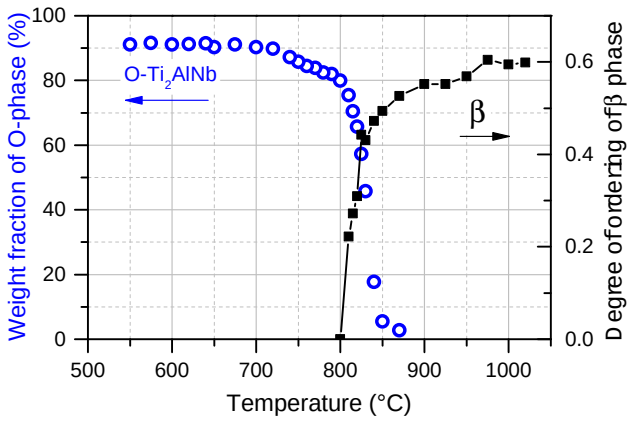

Figure 7: O-phase fraction and the degree of long-range order of β phase during in situ cooling of 10 °C min^{-1} from 1020 °C obtained using Rietveld refinement of X-ray data.

occurs rapidly from around 870 °C to a complete disordering at 800 °C. This fast β phase disordering was accompanied by a two step increase in O-phase fraction: (i) fast transformation of partially ordered β into O (between 870 and 800 °C) followed by (ii) slow transformation of β into O (from 800 °C). At the end of cooling the respective weight fractions of O and β were around 90 and 10 wt. %.

O-phase fraction could be estimated as well from dilatometric data acquired simultaneously with those of X-ray diffraction. The change in relative length of the sample during the cooling from 1020 °C is shown in Figure 8a. Two quasi-linear segments can be clearly seen: for temperature higher than 850 °C and for temperature below 800 °C. According to X-ray data previously discussed, the high temperature range corresponds to the β domain while low temperature range to the β + O domain. Therefore, the transition between one linear part to the other corresponds to increase in O-phase fraction, which can be estimated using a lever rule from dilatometric data and taking into account that 90 wt. % of O is formed at the end of experiment, according to X-ray diffraction. The comparison of O-phase fraction thus estimated from dilatometric data to the one obtained from X-ray data shows a good agreement at the beginning of O-phase formation. From 45 wt. % of O phase formed a difference is observed: the kinetics given by dilatometry is slower than that obtained from X-ray diffraction (Figure 8b). Moreover, O-phase almost reached stable fraction at around 750 °C, according to X-ray diffraction, while it continued to form according to dilatometry. Such a disagreement between dilatometry

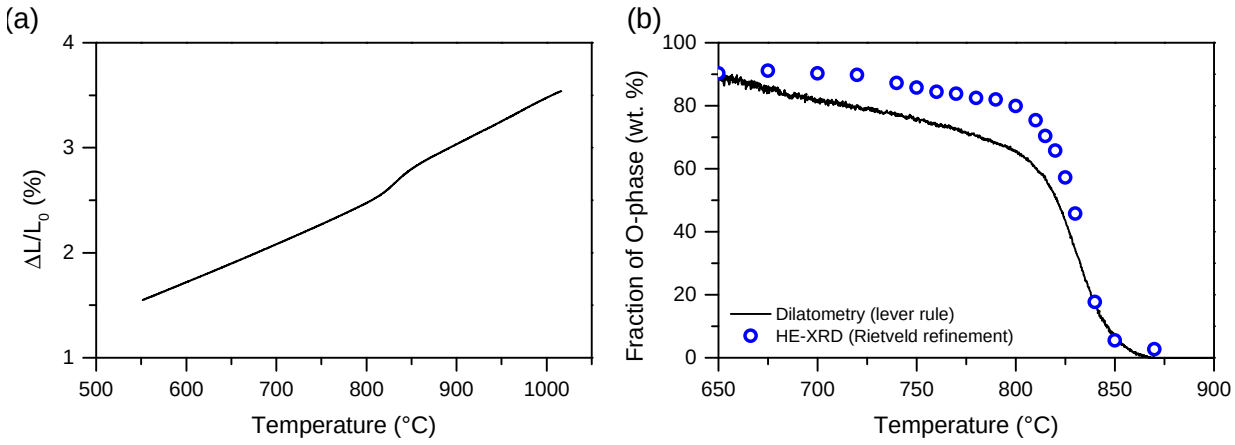

Figure 8: Comparison of results obtained on cooling from 1020 °C with a rate of 10 °C min^{-1} from dilatometric data and those of X-ray diffraction: (a) change in relative length of the sample recorded on cooling and (b) fraction of O-phase obtained by Rietveld refinement of diffractograms and estimated using lever rule from dilatometric data.

and X-ray data should be related to complex phenomena occurring during the O-phase formation resulting in sample volume variation which is not proportional to the O-phase fraction.

Coefficients of thermal expansion for different temperature ranges are deduced from fitting linear segments to the curve presented in Figure 8a and are summarized in Table 3. For β domain (between 1020 and 870 °C), a linear thermal contraction was observed with the coefficient of thermal expansion in agreement with that of β phase obtained using lattice parameter from Rietveld refinement of X-ray data (Figure 9). It is interesting to note that the formation of O-phase leads to an increase in β lattice parameter which further decreases once the O-phase formation is slowed down. Such variations in β lattice parameter suggest the evolution of the chemical composition during O-phase formation [36]. Such an evolution is remarkably important during the first stage when partially ordered β transforms into O-phase.

3.3 Electrical resistivity

The electrical resistivity of the studied Ti2AlNb alloy for different temperatures measured on cooling from 1020 °C with a rate of 10 °C min^{-1} is shown in Figure 10. In the

Table 3: Coefficient of thermal expansion of studied Ti2AlNb alloy obtained from dilatometric data for different temperature ranges.

Temperature range (°C)	Phases	Coefficient of thermal expansion (K^{-1})
550-750	β + O	3.6×10^{-5}
870-1020	β	4.4×10^{-5}

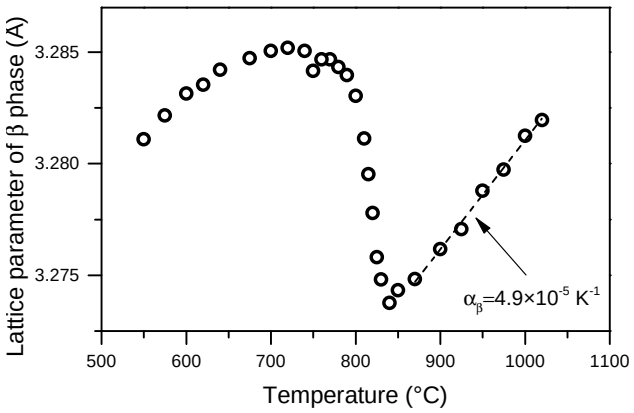

Figure 9: Lattice parameter of β phase for different temperatures obtained from Rietveld refinement of X-ray data recorded on cooling from 1020 °C with a rate of 10 °C min^{-1}. The value of corresponding coefficient of thermal expansion of β in the temperature range from 870 to 1020 °C is given.

high temperature range (above 850 °C) where only partially ordered β phase exists, the resistivity increases with temperature decrease. In the absence of phase transformations, the electrical resistivity is known to decrease with temperature. Therefore, one can speculate that a phase transition could occur when the temperature was decreased from 1020 to 850 °C. The results obtained from X-ray data suggested decrease of degree of ordering of the β phase during cooling in high temperature domain. Order→disorder transition is known to induce an increase in electrical resistivity. Therefore, increase in electrical resistivity on cooling from 1020 to 850 °C might be explained by disordering of β phase.

Around 850 °C an abrupt decrease of electrical resistivity is observed associated to β transformation into O-phase (Figure 10). After a fast resistivity decrease, it decreased slowly when ordering had completely disappeared confirming the two stages of O-phase formation with two different kinetics: (i) fast kinetics for partially ordered β transformation into O and (ii) slow kinetics for disordered β transformation into O.

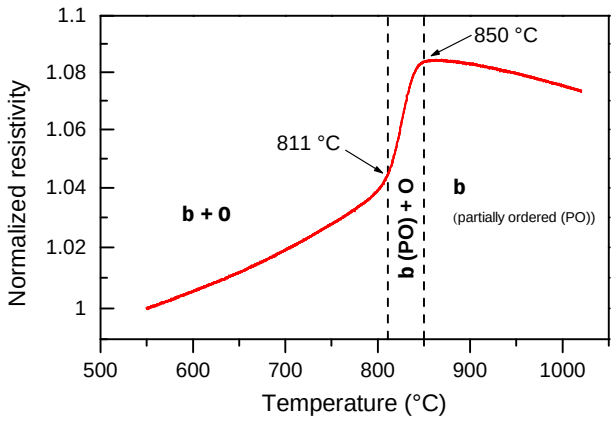

Figure 10: Electrical resistivity of the studied Ti2AlNb alloy for different temperatures measured on cooling from 1020 °C with a rate of 10 °C min^{-1}.

4 Discussion

X-ray diffraction and electrical resistivity give close start temperatures of O-phase formation (the solvus temperature) as well as the temperatures of complete β disordering on cooling (Table 4). However, the X-ray diffraction and dilatometry seem to be more sensitive to detect the very beginning of the O-phase formation. It is worth reminding that X-ray diffraction experiments and resistivity measurements were carried out independently (in different labs with different experimental equipment and at different times).

Table 4: Solvus temperature (°C) for O-phase as well as the disordering temperature of β phase as obtained on cooling 10 °C min^{-1} using X-ray diffraction, dilatometry and electrical resistivity measurements.

Technique used	O-phase solvus (°C)	Temperature of β disordering (°C)
X-ray diffraction	870	800
Electrical resistivity	850	811
Dilatometry	870	-

The microstructure after applied heat cycle, as observed using SEM and backscattered electrons, is shown in Figure 11. As compared with the initial microstructure given in Figure 1, a lot of laths have been formed during the cooling of 10 °C min^{-1}. The data obtained during X-ray diffraction experiments suggest the presence of β and O phases. According to literature data for Ti2AlNb alloys, β phase should be enriched by Nb in comparison with O phase [6]. Therefore, the bright regions in Figure 11 should

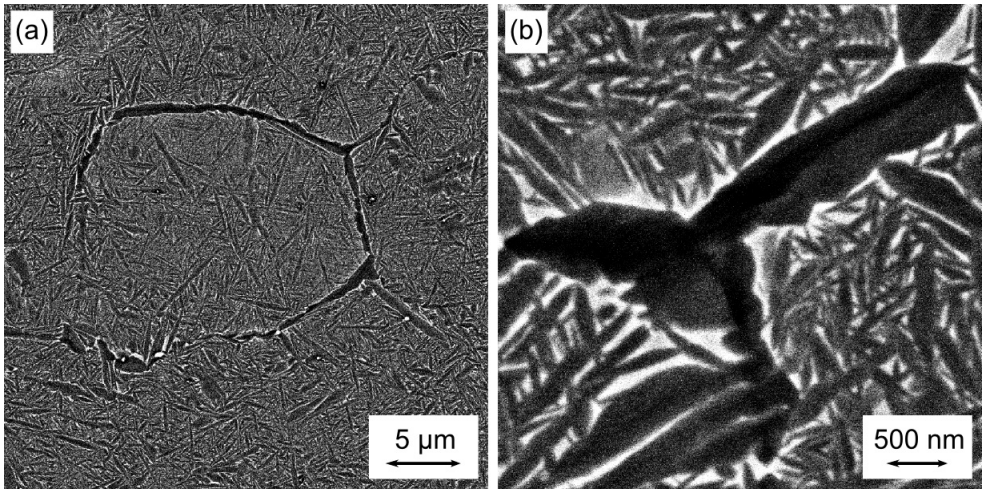

Figure 11: Microstructure of studied Ti2AlNb alloy observed using scanning electron microscope (backstcattered electrons) after cooling from 1020 °C with a rate of 10 °C min^{-1}: (a) overall microstructure and (b) microstructure in the vicinity of former β grain boundaries (β phase in bright, α_2 phase in dark and O-phase in grey).

correspond to β phase while the grey regions should be the O phase. It is worth noting that analysis using energy dispersive spectroscopy in SEM was attempted to evaluate the phase compositions. However, it was not possible to differentiate the precipitates due to their small size. Several dark regions, mainly seen as thin films at former β grain boundaries, and surrounded by grey regions (O phase) can be observed as well in Figure 11b. Ref. [6] reported that α_2 phase had the lowest Nb content as compared to that in β and O phases, and that O phase could form around α_2 precipitates in Ti2AlNb alloys with different Nb/Al ratios [6, 14]. Thus, it can be speculated that the dark precipitates situated at former β grain boundaries corresponded to precipitates of α_2 phase. It might not be detected during high-energy X-ray diffraction experiment due to its slow precipitation kinetics on cooling of 10 °C min^{-1} resulting in low fraction and/or small size (intensive precipitation at grain boundaries corroborates with this hypothesis) in agreement with [15].

Thermodynamic simulations using TCTI2 database were carried out as well for the studied Ti2AlNb alloy. The minor elements such as oxygen, nitrogen and hydrogen were neglected and, for other elements, the contents were taken according to Table 1. Simulation predicts that α_2 phase fraction can reach about 20 wt. % close to 940 °C (Figure 12a)[1].

[1]For thermodynamic simulation, to get convergence, O1_DIS phase had to be rejected.

Such a high phase fraction should be easily quantified using synchrotron X-ray diffraction. Moreover, one can observe as well that, according to thermodynamic simulation, at the temperature of initial isothermal holding of 1020 °C 3 wt. % of α_2 phase might be present in the alloy which is in contradiction with the initial diffractogram obtained on homogeneized material prior to experiments (Figure 4). The thermodynamic simulation gives access as well to the volume evolution of the alloy as function of temperature. Using these data and supposing an isotropic thermal expansion, the linear thermal expansion could be estimated from the Eq. (2) [37]

$$\frac{\Delta L}{L_0} \approx \frac{1}{3}\frac{\Delta V}{V_0}, \tag{2}$$

where $\frac{\Delta L}{L_0}$ is relative length change and $\frac{\Delta V}{V_0}$ is relative volume change; the reference V_0 was taken at 400 °C. The estimation of relative length change of the studied alloy with temperature from thermodynamic data is presented in Figure 12b. The coefficient of thermal expansion in fully ordered β+α_2 temperature range (4.4×10^{-5} K^{-1}) is in a good agreement with that for the temperature range 860-1020 °C obtained from dilatometric data recorded on cooling of 10 °C min^{-1} (4.9×10^{-5} K^{-1}) (Table 3). It is worth noting that expected coefficient of thermal expansion for β alone is approximately two times smaller than that of β and α_2 mixture (Figure 12b).

One can conclude that the contraction observed on dilatometric curve of Figure 8 when O phase started to form is explained by a low molar volume of O phase as compared with that for β and α_2 phases (Figure 12c). It can be seen as well that the calculated molar volume of O phase should increase with temperature decrease resulting in alloy expansion (Figure 12b) when it is cooled in equilibrium conditions. However, it was not possible to confirm or deny experimentally such an unexpected phenomena in the present work due to cooling rate of 10 °C min^{-1} used which could not guarantee equilibrium cooling.

The O-phase composition expected on cooling is quite constant with 25 and 24-27 at. % of Al and Nb, respectively (Figure 12d). The α_2 phase, which is stable in the temperature range from 1030 to 600 °C, is expected to have Al and Nb content vary-

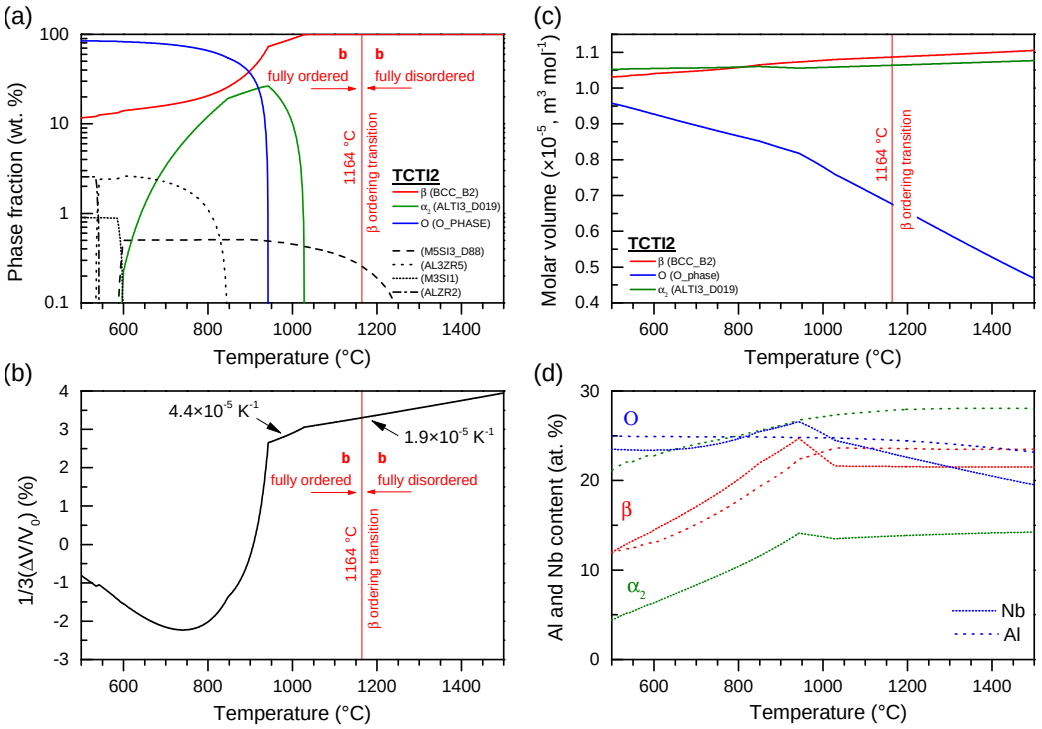

Figure 12: Thermodynamic simulation for the composition of the studied alloy given in Table 1 neglecting O, N and H and using Thermo-Calc software and TCTI2 database giving temperature dependence for: (a) phase fractions, (b) alloy volume change, (c) molar volumes of β, α_2 and O phases and (d) Al and Nb content in β, α_2 and O phases (the phase notations used in TCTI2 database are given in brackets). B2 corresponds to fully ordered β phase while β refers to fully disordered state. The simulation was carried out rejecting O1_DIS phase.

ing from 28 to 21 at. % and from 14 to 5 at. %, respectively. Finally, β composition corresponds to nominal alloy composition in the high temperature range before α_2 phase formation, then Nb content increases from 22 to 25 at. % when α_2 appears, and Al and Nb gradually decrease from 22 to 12 at. % and from 25 to 12 at. %, respectively due to O-phase formation. Therefore, TCTI2 database predicts that O phase has the maximum Nb content and α_2 has the minimum one. It disagrees the literature data where β was reported to be the most enriched in Nb as compared to α_2 and O [5, 6, 11, 13].

Moreover, TCTI2 database clearly separates the existence of ordered (B2) and disordered β: the complete ordering of β occurs at 1164 °C with the decrease of temperature (Figure 12) while the experimental data indicated partial ordering of β on cooling from 1020 to approximately 800 °C (Figure 7 and Table 4). The data available in the literature reported as well the separate existence of fully disordered and fully ordered β. Several studies stated the ordered B2 structure after casting or high temperature annealing [3, 5, 8, 12, 13, 15, 17]. In Ref. [7] a presence of partially ordered β was suggested with low degree of long-range order and a quantitative analysis of degree of long-range order of β phase was attempted in [16]. Refs. [6, 10] suggested composition and temperature dependence of degree of ordering of β phase. Moreover, the ordering transition in β phase was assumed to be a second-order transformation [5, 6]. However, most of these results were obtained using *post mortem* analyses after quenching from high temperature domain speculating thus that no ordering transition could happen on cooling. It makes difficult data interpretation if β phase was partially ordered before quenching. Moreover, lab X-ray diffraction equipment often fails to detect the superlattice peaks of low intensity. In the present work, using high energy X-ray diffraction during in situ heat treatment, a partially ordered β phase was clearly shown. Therefore, we believe that several alloys studied in the previous works could contain as well partially ordered β phase and the ordering was not observed due to the limitations of experimental techniques used for the microstructure analysis.

Summary

The phase transformations in a Ti2AlNb alloy were studied in situ on cooling at 10 °C min^{-1} using synchrotron X-ray diffraction, dilatometry and electrical resistivity. The main results can be summarized as follows:

- Partial ordering of β phase occurs at temperature higher than 800 °C and seems to decrease slowly with the decrease of temperature from 1020 to 870 °C and fast when the O-phase is formed;
- O-phase formation starts at 870 °C and has two distinct kinetic stages: (i) fast kinetics for partially ordered β phase transformation to O-phase (between 870 and 800 °C, according to X-ray diffraction) and (ii) slow kinetics for disordered β to O transformation (below 800 °C);
- O-phase formation is accompanied by a decrease of electrical resistivity and volume of the alloy;
- α_2 phase was not detected by X-ray diffraction, probably, due to its low fraction formed during the cooling at 10 °C min^{-1}.

Acknowledgments

The "Cristal" chair sponsored by Safran is acknowledged for financial support of the present study. Dr. Louise Briez, Dr. Laurane Finet, Dr. Vincent Huleux and, especially, staff of P07 beamline at PETRA III and Andreas Stark (DESY) are gratefully acknowledged for assistance with X-ray diffraction experiments.

Data availability

The raw/processed data required to reproduce these findings cannot be shared at this time as the data also forms part of an ongoing study.

References

[1] M. Peters, J. Hemptenmacher, J. Kumpfert, and C. Leyens. *Structure and Properties of Titanium and Titanium Alloys.* John Wiley & Sons, Ltd, 2005.

[2] J.B. McAndrew and C.R. Simcoe. *Investigation of the Ti-Al-Cb system as a source of alloys for use at 1200-1800 F.* Wright-Patterson Air Force Base, 1960.

[3] D. Banerjee, A.K. Gogia, T.K. Nandi, and V.A. Joshi. A new ordered orthorhombic phase in a Ti3Al-Nb alloy. *Acta Met.*, 36(4):871 – 882, 1988.

[4] W. Chen and J.W. Li. Development of Ti2AlNb Alloys: Opportunities and Challenges. *Adv. Mat. & Proc.*, pages 23 – 27, 2014.

[5] L.A. Bendersky, W.J. Boettinger, and A. Roytburd. Coherent precipitates in the b.c.c./orthorhombic two-phase field of the Ti-Al-Nb system. *Acta Metallurgica et Materialia*, 39(8):1959 – 1969, 1991.

[6] C. J. Boehlert, B. S. Majumdar, V. Seetharaman, and D. B. Miracle. Part I. The microstructural evolution in Ti-Al-Nb O+Bcc orthorhombic alloys. *Met. Mat. Trans. A*, 30:2305–2323, 1999.

[7] X. Ren and M. Hagiwara. Displacive precursor phenomena in Ti–22Al–27Nb intermetallic compound prior to diffusional transformation. *Acta Mat.*, 49(19):3971 – 3980, 2001.

[8] N.V. Kazantseva, S.L. Demakov, and A.A. Popov. Microstructure and plastic deformation of orthorhombic titanium aluminides Ti2AlNb. III. Formation of transformation twins upon the B2/O phase transformation. *The Physics of Metals and Metallography*, 103:378–387, 2007.

[9] N.V. Kazantseva, S.L. Demakov, and A.A. Popov. Microstructure and plastic deformation of orthorhombic titanium aluminides Ti2AlNb. IV. Formation of the transformation twins upon the α_2/O phase transformation. *The Physics of Metals and Metallography*, 103, 04 2007.

[10] A.A. Popov, A.G. Illarionov, S.V. Grib, S.L. Demakov, M. S. Karabanalov, and O.A. Elkina. Phase and structural transformations in the alloy on the basis of the orthorhombic titanium aluminide. *The Physics of Metals and Metallography*, 106:399–410, 2008.

[11] C. J. Boehlert. The phase evolution and microstructural stability of an orthorhombic Ti-23Al-27Nb alloy. *Journal of Phase Equilibria*, 20:101–108, 1999.

[12] K. Muraleedharan, T.K. Nandy, D. Banerjee, and S. Lele. Phase stability and ordering behaviour of the O phase in Ti-Al-Nb alloys. *Intermetallics*, 3(3):187 – 199, 1995.

[13] F.A. Sadi and C. Servant. On the B2→O phase transformation in Ti–Al–Nb alloys. *Materials Science and Engineering: A*, 346(1):19 – 28, 2003.

[14] Y. Huang, Y. Liu, Y. Zhang, and H. Liang. Thermal stability and mechanical properties of Ti–22Al–25Nb alloy with different initial microstructures. *Journal of Alloys and Compounds*, 842:155794, 2020.

[15] P.K. Sagar, D. Banerjee, K. Muraleedharan, and Y.V.R.K. Prasad. High-temperature deformation processing of Ti-24Al-20Nb. *Met. Mat. Trans. A*, 27, 09 1996.

[16] N.V. Kazantseva, V.A. Sazonova, and G.A. Lyzhina. Effect of the annealing temperature on the long-range order in the B2 phase of the Ti-Al-Nb(Zr,Mo) alloy. *The Physics of Metals and Metallography*, 102, 09 2006.

[17] Y. Huang, Y. Liu, C. Li, Z. Ma, L. Yu, and H. Li. Microstructure evolution and phase transformations in Ti-22Al-25Nb alloys tailored by super-transus solution treatment. *Vacuum*, 161:209 – 219, 2019.

[18] C. Xue, W. Zeng, W. Wang, X. Liang, and J. Zhang. Quantitative analysis on microstructure evolution and tensile property for the isothermally forged Ti2AlNb based alloy during heat treatment. *Mat. Sci. and Eng. A*, 573:183 – 189, 2013.

[19] P. Lin, Z. He, S. Yuan, J. Shen, Y. Huang, and X. Liang. Instability of the O-phase in Ti–22Al–25Nb alloy during elevated-temperature deformation. *Journal of Alloys and Compounds*, 578:96 – 102, 2013.

[20] L. Germann, D. Banerjee, J.Y. Guédou, and J.-L. Strudel. Effect of composition on the mechanical properties of newly developed Ti2AlNb-based titanium aluminide. *Intermetallics*, 13(9):920 – 924, 2005. 2nd IRC International TiAl Workshop.

[21] Y. Zhang, Q. Cai, Z. Ma, C. Li, L. Yu, and Y. Liu. Solution treatment for enhanced hardness in Mo-modified Ti2AlNb-based alloys. *Journal of Alloys and Compounds*, 805:1184 – 1190, 2019.

[22] L. Wang, C. Zenk, A. Stark, P. Felfer, H. Gabrisch, M. Göken, U. Lorenz, and F. Pyczak. Morphology evolution of Ti3AlC carbide precipitates in high Nb containing TiAl alloys. *Acta Mat.*, 137:36 – 44, 2017.

[23] L. Song, X. Hu, L. Wang, A. Stark, D. Lazurenko, U. Lorenz, J. Lin, F. Pyczak, and T. Zhang. Microstructure evolution and enhanced creep property of a high Nb containing TiAl alloy with carbon addition. *Journal of Alloys and Compounds*, 807:151649, 2019.

[24] L. Song, F. Appel, L. Wang, M. Oehring, X. Hu, A. Stark, J. He, U. Lorenz, T. Zhang, J. Lin, and F. Pyczak. New insights into high-temperature deformation and phase transformation mechanisms of lamellar structures in high Nb-containing TiAl alloys. *Acta Mat.*, 186:575 – 586, 2020.

[25] M. Dadé, V.A. Esin, L. Nazé, and P. Sallot. Short- and long-term oxidation behaviour of an advanced Ti2AlNb alloy. *Corr. Sci.*, 148:379 – 387, 2019.

[26] V.A. Esin, B. Denand, Qu. Le Bihan, M. Dehmas, J. Teixeira, G. Geandier, S. Denis, T. Sourmail, and E. Aeby-Gautier. In situ synchrotron X-ray diffraction and dilatometric study of austenite formation in a multi-component steel: Influence of initial microstructure and heating rate. *Acta Materialia*, 80:118 – 131, 2014.

[27] H. M. Rietveld. A profile refinement method for nuclear and magnetic structures. *J. Appl. Cryst.*, 2(2):65–71, Jun 1969.

[28] FIT2D, www.esrf.eu/computing/scientific/FIT2D/.

[29] B. W. Levinger. Lattice Parameter of Beta Titanium at Room Temperature. *JOM*, 5:195 – 195, 1953.

[30] D. Banerjee, T.K. Nandy, and A.K. Gogia. Site occupation in the ordered beta phase of ternary Ti-Al-Nb alloys. *Scr. Met.*, 21(5):597 – 600, 1987.

[31] B. Mozer, L.A. Bendersky, W.J. Boettinger, and R.Grant Rowe. Neutron powder diffraction study of the orthorhombic Ti2AlNb phase. *Scr. Met. Mat.*, 24(12):2363 – 2368, 1990.

[32] FullProf Manual, https://www.ill.eu/sites/fullprof/php/tutorials.html.

[33] J. Rodríguez-Carvajal. Recent advances in magnetic structure determination by neutron powder diffraction. *J. Physica B: Cond. Mat.*, 192(1):55 – 69, 1993.

[34] P. Archambault and D. Godard. High temperature precipitation kinetics and ttt curve of a 7xxx alloy by in-situ electrical resistivity measurements and differential calorimetry. *Scripta Materialia*, 42(7):675 – 680, 2000.

[35] S.R. Stock B.D. Cullity. *Elements of X-Ray Diffraction*. Pearson Education Limited, third edition, 2014.

[36] B. Denand, V.A. Esin, M. Dehmas, G. Geandier, S. Denis, T. Sourmail, and E. Aeby-Gautier. Carbon content evolution in austenite during austenitization studied by in situ synchrotron X-ray diffraction of a hypoeutectoid steel. *Materialia*, 10:100664, 2020.

[37] F. G. Caballero, C. Capdevila, and C. García De Andrés. Modelling of kinetics of austenite formation in steels with different initial microstructures. *ISIJ Int.*, 41(10):1093–1102, 2001.